





Title	The Anti-Tumor Effects of M1 Macrophage-Loaded Poly (ethylene glycol) and Gelatin-Based Hydrogels on Hepatocellular Carcinoma
Author(s)	Guerra, AG; Yeung, WH; Qi, X; Kao, WJ; Man, K
Citation	Theranostics, 2017, v. 7 n. 15, p. 3732-3744
Issued Date	2017
URL	http://hdl.handle.net/10722/248580
Rights	Theranostics. Copyright © Ivyspring International Publisher.; This work is licensed under a Creative Commons Attribution-NonCommercial-NoDerivatives 4.0 International License.


Research Paper

The Anti-Tumor Effects of M1 Macrophage-Loaded Poly (ethylene glycol) and Gelatin-Based Hydrogels on Hepatocellular Carcinoma

Alberto Daniel Guerra^{1*}, Oscar W.H. Yeung^{2*}, Xiang Qi², W. John Kao^{1, 3}, Kwan Man²

1. School of Pharmacy, Division of Pharmaceutical Sciences, Pharmacy Practice Division, University of Wisconsin-Madison, 777 Highland Avenue, Madison, WI 53705, USA;
2. Department of Surgery, The University of Hong Kong, Pokfulam, Hong Kong SAR; Collaborative Innovation Center for Diagnosis and Treatment of Infectious Diseases, China;
3. Chemical Biology Centre, The University of Hong Kong, Pokfulam, HKSAR.

* Co-First Authors

 Corresponding authors: Kwan Man, Department of Surgery, LKS Faculty of Medicine, The University of Hong Kong, L9-55, 21 Sassoon Road, Hong Kong SAR Tel: +852-39179646; Fax: +852-39179634; E-mail: kwanman@hku.hk W. John Kao, Chemical Biology Centre, The Hong Kong Jockey Club Building for Interdisciplinary Research, 5 Sassoon Road, The University of Hong Kong, Pokfulam, Hong Kong SAR Tel: +852 2219 4664; Fax: +852 2559 9315; Email: wjkao@hku.hk

© Ivyspring International Publisher. This is an open access article distributed under the terms of the Creative Commons Attribution (CC BY-NC) license (<https://creativecommons.org/licenses/by-nc/4.0/>). See <http://ivyspring.com/terms> for full terms and conditions.

Received: 2017.03.24; Accepted: 2017.07.03; Published: 2017.08.23

Abstract

Background and Aims: Recently we reported that direct injection of M1 macrophages significantly caused tumor regression *in vivo*. Despite the promising result, a major limitation in translating this approach is the induction of acute inflammatory response. To improve the strategy, a biocompatible scaffold for cell presentation and support is essential to control cell fate. Here, we aimed to elucidate the anti-tumor effects of a poly(ethylene glycol) diacrylate (PEGdA) and thiolated gelatin poly(ethylene glycol) (Gel-PEG-Cys) cross-linked hydrogels encapsulated with M1 macrophages in both *in vitro* and *in vivo* disease models.

Methods: Hydrogels were made at 0.5% (w/v) Iragcure 2959 photoinitiator, 10% (w/v) PEGdA, and 10% (w/v) Gel-PEG-Cys. Monocytic THP-1 cells were loaded into hydrogels and differentiated into M1 macrophages with lipopolysaccharide (LPS) and interferon gamma (IFN- γ). The M1 hydrogels were then cocultivated with HCC cell-lines Hep3B and MHCC97L to investigate the anti-tumor capacities and the associated molecular profiles *in vitro*. A nude mice ectopic liver cancer model with dorsal window chamber (DWC) and a subcutaneous tumor model were both performed to validate the *in vivo* application of M1 hydrogels.

Results: M1 hydrogels significantly decreased the viability of HCC cells (MHCC97L: -46%; Hep3B: -56.9%; $P < 0.05$) compared to the control *in vitro*. In response to HCC cells, the hydrogel embedded M1 macrophages up-regulated nitrite and tumor necrosis factor alpha (TNF- α) activating caspase-3 induced apoptosis in the tumor cells. Increased tumor necrosis was observed in DWC filled with M1 hydrogels. In addition, mice treated with M1 hydrogels exhibited a significant 2.4-fold decrease in signal intensity of subcutaneous HCC tumor compared to control ($P = 0.036$).

Conclusion: M1 hydrogels induced apoptosis in HCC cells and tumor regression *in vivo*. Continuous development of the scaffold-based cancer immunotherapy may provide an alternative and innovative strategy against HCC.

Key words: Hepatocellular carcinoma, M1 hydrogels, M1 macrophages, Hydrogels, Animal Model.

Introduction

Hepatocellular carcinoma (HCC) is the fifth most commonly diagnosed malignancy and the second most common cause of death from cancer worldwide. The high metastatic rate and fatality of the disease (overall mortality to incidence ratio >90%) represents a major health issue. Currently, curative treatment options, including surgical and radiofrequency ablation, are only applied to the patients with limited tumor burden¹. Conventional chemotherapy has no significant impact on advanced HCC. As one of the predominant risk factors is sustained inflammation induced by chronic hepatitis or fibrosis, it is highly believed that the altered inflammatory milieu contributes significantly to the tumorigenesis progress. Therefore, combating the disease through an immunological interface is provocative as a novel therapeutic alternative.

Cell-based immunotherapies are rapidly emerging as a promising treatment for many cancers in the last decade. Immunological cells including T cells, natural killer (NK) cells and dendritic cells have been experimented in clinical trials². Adoptive T cell transfer through the isolation and reinfusion of T lymphocytes into patients has shown anti-tumor potential against lymphoid leukemia³⁻⁵. NK cells can be activated to produce abundant amounts of TNF- α and other inflammatory cytokines for the treatment of acute myeloid leukemia, non-Hodgkin lymphoma, and ovarian cancer⁶⁻⁸. Due to the absence of tumor antigens and poor immunogenic tumor environment, most of these immunological cells require additional immuno-editing and *ex vivo* stimulation before further clinical applications. On the other hand, it is now widely believed that tumorigenesis is orchestrated by innate cellular mechanisms without the involvement of the adaptive immune system⁹.

Being a key member of the innate immunity as well as antigen presenting cells, macrophages with different heterogeneities exert opposing functions influencing the fate of tumor development and progression¹⁰. In particular, tumor associated macrophages displaying the Th2 phenotype (M2) have significant roles in orchestrating tumor growth and metastasis. In contrast, the Th1 counterpart (M1) possesses pro-inflammatory and tumor suppressive properties. Accumulating evidences have shown that M1 macrophages can induce tumor rejection in various tumor models¹¹. In our recent study, we revealed the absence of tumoral M1 macrophages in HCC patients¹². Further *in vitro* and *in vivo* studies showed that the M1 populations suppressed HCC cells growth and induced liver tumor regression. Mice

injected with M1 macrophages through portal vein injection exhibited a significant 2.79 fold reduction in tumor volume. Despite its anti-tumor effectiveness, acute inflammation leading to mortality was observed. It was speculated that such approach was highly inflammatory thus necessitate further modification for therapeutic development. The direct injection approach also lacks the ability to controllably retain the immune cells in the tumor site. Therefore, a biocompatible scaffold for cell retaining and localization of the released molecules is essential to improve such cell-based immunotherapeutic approach.

Hydrogels are three-dimensional polymeric and hydrophilic networks which have been widely used for cell encapsulation and controlled release of therapeutic proteins, peptides, drugs and nucleic acids¹³. In addition, the biomaterial has also been widely utilized to reconstitute 3D culture environment for studying cell-cell interactions and drug screening in various cancer models¹⁴. A thiolated gelatin poly(ethylene glycol)(Gel-PEG-Cys) and poly(ethylene glycol) diacrylate (PEGdA) cross-linked hydrogel was selected as a biomimetic scaffold for local delivery of activated M1 macrophages. PEG exhibits desirable biomedical properties such as protein resistance, low immunogenicity, and enhanced biocompatibility while gelatin contains cell-binding motifs, such as RGD oligopeptides, which support cell adhesion and proliferation. The physical characteristics of the biomaterial including stiffness, swelling, enzymatic degradation, 2D cell adhesion and 3D cell encapsulation were studied in details previously¹⁵⁻¹⁶. In terms of biological functions, we have reported that these PEG-hydrogels loaded with mesenchymal stromal/stem cells (MSCs) leads to spatially and temporally controlled cellular presentation to wound sites while maintaining pluripotency and a favorable healing outcome¹⁷⁻²⁰. The encapsulated MSCs demonstrate extensive cytoplasmic spreading, the formation of cellular networks, and improved focal adhesion with the co-cultured of macrophages¹⁷⁻¹⁹. Apart from displaying the active immunogenic effects and biocompatibility, the hydrogels have been shown to be a bio-scaffold permitting the release of the entrapped cells derived small molecules and cytokines to the surrounding environment²¹⁻²³. With such evidences, we speculate that the PEG-hydrogels is an ideal candidate for retaining M1 macrophages as well as exerting its tumor suppressive functions for our study.

By surrounding tumors with M1 hydrogels, we hypothesized that tumor regression might be resulted similar to the previous direct injection approach but with less adverse effects. Despite the significances of innate immunology in tumorigenesis, there is a lack of evidences elucidating the tumor killing capacities of innate cells based hydrogels. In the present study, we first validated the biocompatibility of the hydrogels for M1 macrophages and then investigated the anti-tumor potential of M1 macrophage-loaded PEG hydrogels on HCC tumoral cell-lines. Two HCC animal models including the real time intravital imaging system for examining tumor regression were employed. Furthermore, the M1 hydrogel derived molecules responsible for the tumor suppressive phenotypes were identified. With these evidences, we have developed a potential biomaterial platform to safely delivering and sustaining M1 macrophages for further developing such cell-based immunotherapy for cancer treatment.

Materials and Methods

Cell culture

The human acute monocytic leukemia cell line THP-1, normal hepatic cell line MIHA and HCC cell lines were purchased from ATCC and maintained according to ATCC guidelines. For luciferase-labeling, MHCC97L (a kind gift from Liver Cancer Institute, Fudan University) cells were transfected with luciferase gene in pGL3 vector (Promega), and positive clones were selected according to luciferase activity in Xenogen *In vivo* Imaging System 100 (Xenogen IVIS® 100, Xenogen Corporation).

Hydrogel synthesis

PEGdA/Gel-PEG-Cys composite hydrogel was synthesized following previously procedures with modifications¹⁵⁻¹⁶. PEGdA was synthesized via acrylation of PEG-diol (MW 2kDa, Sigma-Aldrich) by reacting a dichloromethane (DCM) solution of PEG-diol with acryloyl chloride and triethylamine at a relative molar ratio of 1:4:4. The raw product was filtered with aluminum oxide and washed three times with 1N NaOH and the final product was precipitated in cold diethyl ether, dried under vacuum for at least 2 days, and analyzed via reverse phase high performance liquid chromatography (10-100% acetonitrile at 1mL/min, elution time 13.2 minutes) and NMR for acrylation percentage (acrylation peaks at 6.0PPM). Only PEGdA with an acrylation percentage of 80% or more was used for this study. Gel-PEG-Cys was synthesized using N-hydroxysuccinimide-functionalized PEG

(Bis-NHS-PEG) synthesized from via carbonate linkaged between PEG-diol (MW 2kDa, Sigma Aldrich) and N,N'-disuccinimidyl carbonate with 4-(dimethylamino)pyridine as a catalyst. Gelatin was modified with L-cysteine by dissolving Bis-NHS-PEG (1.0g, 0.43mmol) in 5mL of dry N,N-dimethylformamide. L-cysteine (0.08g, 0.66mmol) was added to the Bis-NHS-PEG solution followed by addition of 110µL DIPEA. The reaction was kept under argon for 20 minutes then 1% gelatin (type B, 75 bloom, from bovine skin, Electron Microscopy Sciences, Hatfield, PA) in PBS solution was added (60mL) followed by a 1 hour stir at room temperature under argon protection at a pH of 8.0. The product was dialyzed (6-8kDa cutoff) for 2 days against double-distilled water and filtered through a 0.22µm filter, snap frozen and lyophilized followed by analysis via NMR (thiol groups at 1.3PPM) and analysis of relative free thiol concentration via the Ellman test.

M1 hydrogel preparation

Hydrogel formulations were made in PBS to synthesize a 0.5% (w/v) Irgacure 2959 photoinitiator (BASF, Ludwigshafen, Germany), 10% (w/v) PEGdA and 10% (w/v) Gel-PEG-Cys sterile-filtered solution prepared and characterized as described previously^{15-16, 24}. The procedures for the preparation of M1 hydrogels used *in vitro* and *in vivo* studies was illustrated (**Figure 1**). For *in vitro* studies, a THP-1 cell suspension was added into the formulation at the desired number of cells. The formulations were then pipetted (100µL) into a 10mm glass-bottom Petri dish (*In vitro* Scientific) with a circular recess and then polymerized by exposing to UV light (λ_{\max} =365nm, 100W/cm²) for 2 minutes. For M1 polarization, culture medium containing 640nM PMA was added to each dish incubated at 37°C for 6 hours and then 150ng/mL LPS and 25ng/mL IFN-γ for another 18 hours. M1 hydrogels were then transferred to experimental wells or inserts for further assays. For *in vivo* studies, THP-1 cells were polarized into M1 macrophages prior to loading to hydrogels and experimentation on tumor bearing mice.

M1 characterization in hydrogels

For visualizing the hydrogel embedded macrophages, a monoclonal mouse anti-human CD68 FITC antibody (1:100; Dako) was applied with standard immuno-fluorescent staining protocol. Afterwards, the stained population in hydrogels was observed through 2D and 3D-images reconstruction under CZ LSM 710 confocal system.

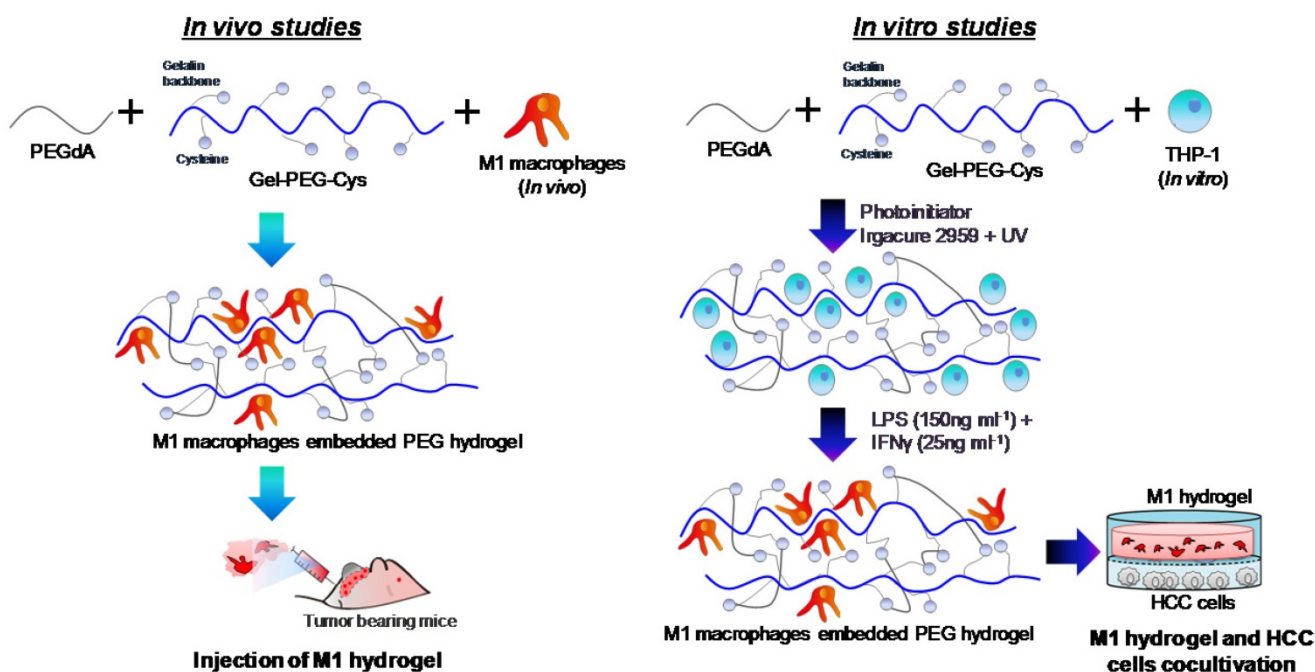


Figure 1. Schematic diagram illustrating the preparation of M1 hydrogel for *in vivo* and *in vitro* studies.

Cytokine antibody array analyses

The expression profiles of 12 different cytokines (Th1/Th2/Th17) in culture (M1 hydrogel, MIHA, MHCC97L and Hep3B) and coculture (M1 hydrogel-MHCC97L, M1 hydrogel-Hep3B, M1 hydrogel-MIHA) conditioned supernatants were determined using antibody based PathScan® Th1/Th2/Th17 Cytokine Antibody Array Kit (Cell Signaling). All procedures were performed according to the manufacturer's instructions.

In vitro treatment of HCC cells with M1 macrophage-loaded hydrogels

The treatment of M1 hydrogels to HCC cells was conducted using the non-contact coculture transwell system (Corning). THP-1 cells were added at the desired number in 100 μ l hydrogel and polarized to M1 macrophages as described above. After polarization, each M1 hydrogel was transferred to 10mm 0.4- μ m sized pores inserts and to 24-well cell culture plate seeded with MHCC97L, Hep3B or MIHA cell-lines (1×10^5 cells per well). Co-cultures were either conducted at various M1 macrophage concentrations for 4 days, or for 1-4 days at 5×10^5 M1 macrophages/hydrogel. After co-culture, the supernatants were stored for analysis, and a LIVE/DEAD® (Invitrogen) stain was applied to the cells with subsequent imaging on a Nikon Eclipse TE300 microscope. Metabolic activities of the treated cells were determined using an MTT metabolic activity assay (Acros Organics). Briefly, a 5mg/mL

solution of thiazolyl blue tetrazolium bromide in PBS was added to media at 10 μ L/mL and 1mL of the MTT media was added to each well and incubated at 37°C for 4 hours. Followed by the removal of the media, stained cells were solubilized with 1mL of DMSO on a plate shaker for 10 minutes and quantified via optical density at 570nm.

Measurement of nitrite, IL-6 and TNF- α production

Nitrite measurements were performed using the Griess reagent (G4410; Sigma) according to the manufacturer's recommendation. Supernatants collected from co-cultures were incubated with a 1:1 ratio with Griess reagent. After incubation for 15 minutes, the plate was read on a spectrophotometer at 540nm. With a standard curve, the nitrite concentration for each culture supernatant was determined. The level of IL-6 and TNF- α in each culture supernatant were also analyzed using Duoset® ELISA kits with corresponding assay antibodies (R&D Systems, Inc.).

In vitro treatment of HCC cells with TNF- α , IL-6 and nitrite

1×10^5 Hep3B, MHCC97L, and MIHA cells were treated with 850pg/mL recombinant IL-6 (R&D Systems, Inc.), 1,250pg/mL recombinant TNF- α (R&D Systems, Inc.), or 250nM nitrite (Absolute Standards, Hamden, CT) for 24 hours similar to their secretory level found in previous co-culture experiments. Cells were then stained and imaged with LIVE/DEAD®

stain followed by MTT metabolic activity assay.

Gene expression analyses

RNA was isolated from the treated Hep3B, MHCC97L, and MIHA cells by lysing the cells with 0.5mL of TRIzol reagent (ThermoFisher Scientific). For the hydrogel embedded M1 macrophage, M1 hydrogels were placed in liquid nitrogen and crushed into powder followed by the addition of TRIzol reagent. Followed by standard RNA isolation protocol using RNeasy Mini Kit (Qiagen), the total RNA was then reverse transcribed with iScript™ cDNA synthesis kit (Bio-Rad) with the iCycler thermocycler (Bio-Rad). RT-PCR was performed on synthesized cDNA using a StepOnePlus Real-Time PCR System (ThermoFisher Scientific) using TaqMan Expression Assay Probes for *IL-6*, *TNF- α* , *IDO1*, and *caspase-3*. Data pertaining to mRNAs were collected quantitatively and the CT number was corrected by CT readings of the corresponding internal control glyceraldehyde 3-phosphate dehydrogenase (*GAPDH*).

Western blot

Proteins from HCC cell-lines were prepared using RIPA buffer (50mM Tris-HCl, 1mM EDTA, 0.1% SDS, 150mM NaCl, 1% NP40, 0.1% sodium-deoxycholate, pH 8.0). 10 μ g of protein lysates was separated by 12.5% SDS-PAGE and transferred to PDMF membrane (Millipore). After blocking with 5% non-fat milk, the membrane was incubated with caspase 3 (8G10), cleaved caspase 3 (Asp175) and cleaved PARP (Asp214) (Cell signaling) at 4°C for 16 hours. A secondary antibody against goat (Santa Cruz Biotech) and rabbit (Cell signaling) IgG diluted 1:3000 was added at room temperature for 1 hour. Corresponding band was revealed using the enhanced chemiluminescence system (GE healthcare Amersham Bio-sciences) and monitored with an LAS-1000 (FijiFilm). β -actin was used as a loading control.

Real-time intravital imaging using dorsal window chamber implantation

All animal studies were conducted according to the Animal Ordinance (Control of Experiments, Hong Kong) and the Institute's guidance on animal experimentation. Detailed surgical procedures were as described previously²⁵. Briefly, the dorsal window chamber (DWC) consists of two titanium frames that bind together to form a saddle on the back of the nude mice and is attached using spacers, bolts and fastening nuts. A 'chamber' is formed after a transparent glass cover slip placed onto the attached saddle covering the exposed fascia containing vessels and secured using a sterile removable 'C' clip. The

nude mice ectopic liver cancer model was established using HCC cells (MHCC97L). MHCC97L cells were labeled with fluorescence reporter (GFP) during transduction and then injected subcutaneously into the DWC from the opposing side to the glass cover-slip. 100 μ L of hydrogel containing either PBS or 1 \times 10⁶ fluorescence labeled activated M1 macrophages was then injected directly adjacent to tumor nodule in DWC.

The tissue structure surrounding the tumor nodule, such as collagen, was visualized through two photons secondary harmonic generation. The process of cancer cells invasiveness as well as the hydrogel embedded macrophages was kinetically observed through 3D-images reconstruction under CZ LSM 710 confocal system. The excitation wavelength was 800nm (two-photon system). The emission wave lengths of GFP from tumor cells were 500-550nm. The emission wave lengths from connective tissue and M1 macrophages in hydrogels were 385-425nm. The objective lens was 20X.

Tumor xenografts in BALB/c nude mice and hydrogels implantation

Male athymic nude mice (BALB/c nu/nu, 4-6 weeks old) were used for the subcutaneous tumor animal model. Surgical procedures were as described previously¹². Briefly, 2 \times 10⁶ MHCC97L cells tagged with luciferase, suspended in 0.2mL DMEM, were injected subcutaneously into the flanks of the mice. After 3 weeks of injection as the size of tumor reached approximately 3mm, the mice were divided into 3 groups (Negative control: DMEM; Blank: hydrogel with PBS; M1 gel: hydrogel embedded with 1 \times 10⁶ M1 macrophages; each group with 4 mice). 200 μ L of hydrogel was injected directly adjacent to tumor nodule weekly in the blank and M1 hydrogel group. Followed by the treatment, the tumor size of MHCC97L xenograft was monitored weekly by PE IVIS Spectrum *in vivo* imaging system (PerkinElmer). All mice were euthanized at week 4 and the size of tumor was measured and compared.

Statistical analysis

Comparisons of quantitative data between two groups were analyzed by unpaired Student's t-test. P<0.05 was considered statistically significant with P<0.05 (*), P<0.01 (**). All analyses were performed with Graphpad Prism 5.0.

Results

Characterization of PEG-hydrogel embedded M1 macrophages

Stimulated with LPS and IFN- γ , hydrogel embedded THP-1 cells displayed macrophage marker

CD68 with even cell distribution analyzed by 3D confocal microscopy (Figure 2A, Supplemental Video 1). Identical pro-inflammatory cytokine profiles between M1 macrophages culture and M1 hydrogels were validated as secretory IFN- γ , TNF- α , and IL-8 were found in both conditioned supernatants (Figure 2B). Apart from cytokines, M1 derived nitrites, was also detected in both supernatants from M1 macrophages culture (25 μ M) and M1 hydrogels (15 μ M) (Figure 2C). These data suggested that PEG-hydrogel permitted cell activation, retained the immuno-phenotypes and functions of the M1 populations.

Proliferation suppressive effect of M1 hydrogels on HCC cells but not MIHA cells

With the treatment of M1 hydrogels, decreased viability of HCC cells in a dose and time dependent manner were observed. For the dose effect, hydrogels loaded with 5 $\times 10^5$ and 1 $\times 10^6$ M1 macrophages significantly reduced HCC cell metabolic viability (Hep3B: -31%; MHCC97L: -56%. $P < 0.01$) and (Hep3B: -50%; MHCC97L: -64%. $P < 0.01$) respectively compared to controls after 4 days of co-culture (Figure 3A-D). For the time effect, hydrogels loaded with 5 $\times 10^5$ M1 macrophages significantly reduced viability of Hep3B (2 days: -31%; 3 days: -42%; 4 days: -53%. $P < 0.01$) and MHCC97L (2 days: -29%; 3 days: -37%; 4 days: -62%. $P < 0.01$) compared to controls after co-culture (Supplemental Figure 1A-D).

In contrast to HCC cells, hydrogels loaded with 5 $\times 10^5$ M1 macrophages had no significant impact on normal hepatic cell line MIHA in terms of viable growth density (Figure 3E) and metabolic activity (Figure 3F). Taken together, we demonstrated that treatment of M1 hydrogel (5 $\times 10^5$ cells; 4 days) specifically suppressed HCC cells viabilities but not hepatocyte cells (Figure 3G).

Cytokine profiling and molecular analysis of HCC, MIHA and M1 hydrogels co-cultures

To identify potential tumor suppressive cytokines derived from M1 hydrogels, cytokine array analysis were performed. Similar to M1 macrophages culture and M1 hydrogels, we first confirmed that the biomaterials had no effects on HCC cells in terms of cytokine secretion (Figure 2B and 4A). Importantly, supernatants of Hep3B and MHCC97L cells treated with M1 hydrogels (5 $\times 10^5$ cells, 4 days) showed increase pro-inflammatory cytokines of IL-6 and TNF- α compared to non-treatment groups (Figure 4A). Further ELISA analysis revealed that by increasing the number of M1 macrophages to 1 $\times 10^6$ per hydrogel, higher levels of IL-6 and TNF- α in the coculture supernatants were detected ($P < 0.01$) (Figure 4B).

In addition, M1 hydrogels (5 $\times 10^5$ and 1 $\times 10^6$) induced the level of nitrite in the co-culture supernatants (Figure 4B). Apart from the dose effect, increased the incubation time of M1 hydrogels with HCC cells also induced IL-6, TNF- α , and nitrite in the co-culture supernatants (Figure 4C-D). Higher levels of IL-6, TNF- α , and nitrite in the co-culture supernatant of MIHA cells with M1 hydrogels were also observed (Figure 4E).

Anti-tumor potentials of the identified M1 hydrogel derived molecules

Based on these findings, we further examined the tumor suppressive capacities of the identified molecules derived from M1-hydrogels. Using the concentrations consistent to previous ELISA analysis, treatment of Hep3B and MHCC97L cells with 1250pg/mL TNF- α (Hep3B: -51%; MHCC97L: -33%. $P < 0.01$) or 250nM nitrite (Hep3B: -39%; MHCC97L: -13%. $P < 0.01$) for 24 hours demonstrated significant decrease in metabolic viability compared to untreated controls (Figure 5A-D). In contrast, similar treatment

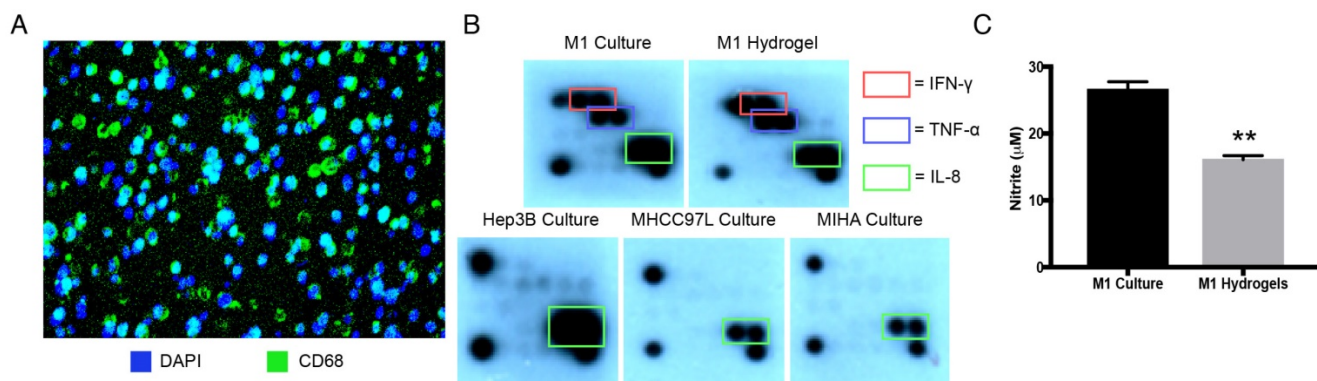


Figure 2. Characterization of M1 hydrogels. (A) Cross section of hydrogels loaded with differentiated THP-1 cells that were CD68 positive (green) with the nuclei stained with DAPI (blue). (B) Cytokine secretion profiles of M1 macrophages, M1 hydrogel, Hep3B, MHCC97L and MIHA cell culture supernatants. (C) Nitrite level in M1 macrophages culture and M1 hydrogel supernatants. The error bar represented as SD. ** $P < 0.01$.

of nitrite to MIHA cells had no effect on metabolic viability but a significant decrease of the cell viability treated with TNF- α or 852pg/mL IL-6 were observed (Figure 5E-F).

Anti-tumor molecular mechanism of M1 macrophage-loaded hydrogels

In response to HCC cells, transcript analysis showed that hydrogels embedded M1 macrophages up-regulated *TNF- α* (Hep3B: 9.5 fold increase, $P=0.0128$; MHCC97L: 10.2 fold increase, $P=0.0107$), *IL-6* (Hep3B: 5.8 fold increase, $P=0.002$; MHCC97L: 5.8 fold increase, $P=0.0093$) and *IDO1* (Hep3B: 2.7 fold increase, $P=0.0061$; MHCC97L: 2.3 fold increase, $P=0.0487$) compared to untreated controls (Figure 6A).

With the presence of M1 hydrogels, Hep3B cells up-regulated *IL-6* (4.9 fold increase, $P<0.0001$), *TNF- α* (5.6 fold increase, $P=0.0075$) and *caspase-3* (2.6 fold increase, $P=0.0221$). MHCC97L cells with similar treatment demonstrated a significant increase in *IL-6* (57.4 fold increase, $P=0.0005$) and *caspase-3* (2.4 fold increase, $P=0.0014$) expression (Figure 6B-C). Interestingly, MIHA cells demonstrated a significant increase in *TNF- α* (4.9 fold increase, $P=0.0232$) and *IL-6* but not *caspase-3* upon the treatment with M1 hydrogels (Figure 6D). Further western blot analysis

revealed that M1 hydrogels induced the activation of apoptotic caspase-3 and PARP in cleaved form in Hep3B and MHCC97L cells (Figure 6E).

In vivo anti-tumor efficacy of M1 hydrogels

To investigate the tumor suppressive potentials of M1 hydrogels, two animal models were applied. First, the ectopic nude mice liver cancer model with dorsal window chamber was established (Figure 7A). With confocal microscopy, the real time intravital images indicated that less metastasis and more necrotic area in the ectopic liver tumor were observed in the M1 hydrogel group compared to the untreated (negative control) and blank hydrogels group (Figure 7B). Further 3D reconstructed images illustrated the intravital distribution of hydrogel embedded M1 macrophages to the tumor (Figure 7C).

Second, a subcutaneous HCC model for examining the tumor regression capacities of M1 hydrogels was applied (Figure 8A). After 4 weeks of continuous treatment, the intensity of tumor luciferase signals in M1 hydrogel group were significantly decreased by 2.4-fold ($23.2U\pm 5.8$) compared to untreated controls ($54.9U\pm 10.3$) ($P=0.036$) (blank hydrogels group: $48.2U\pm 10.3$) (Figure 8B-C). In terms of tumor volumes, 6.9-fold decrease were also observed in the mice treated with M1

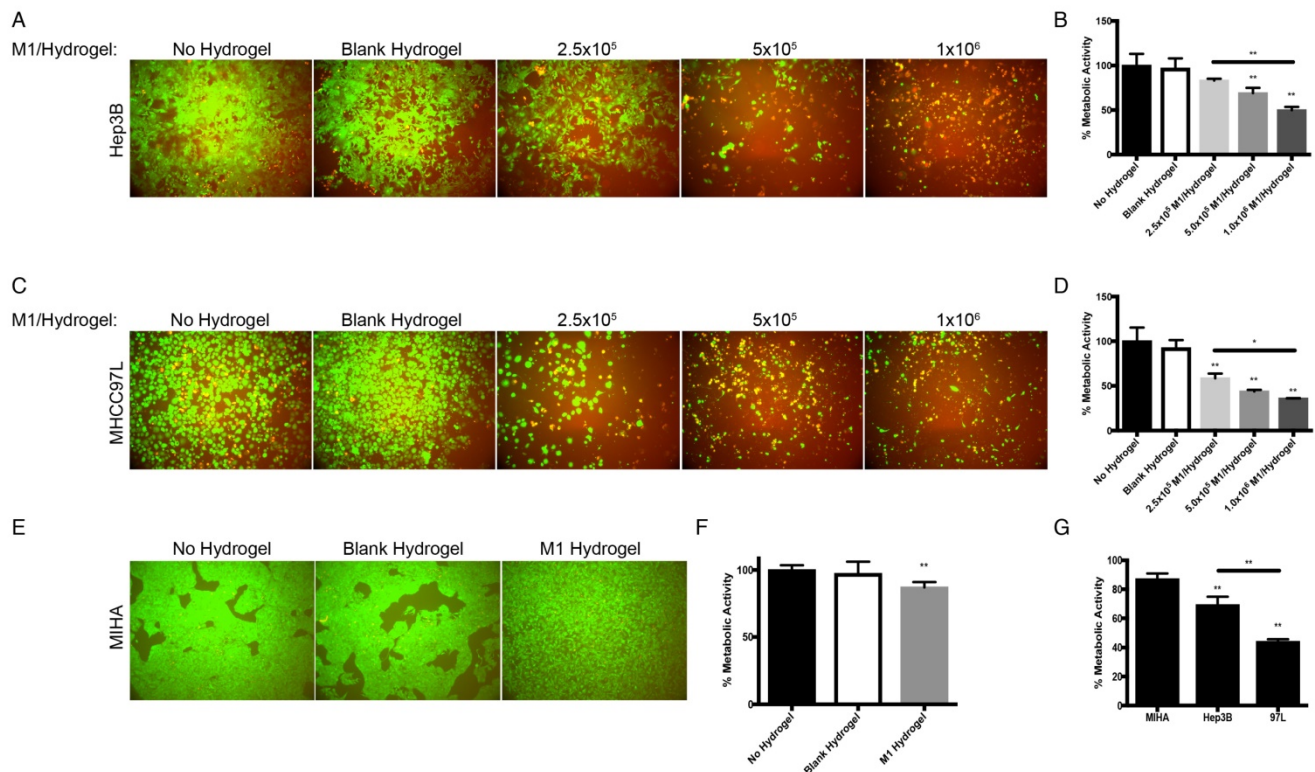


Figure 3. Dose dependent effects of M1 macrophage-loaded hydrogels on HCC and MIHA cells after 4 days of co-culture. (A) Live/dead images of Hep3B cells after the treatment with M1 hydrogels. (B) Corresponding normalized metabolic activity. (C) Live/dead images of MHCC97L cells after the treatment with M1 hydrogels. (D) Corresponding normalized metabolic activity. (E) Live/dead images of MIHA cells after the treatment with M1 hydrogels. (F) Corresponding normalized metabolic activity. (G) Comparison of normalized metabolic activity between MIHA, Hep3B, and MHCC97L cells after the treatments with M1 hydrogels. The error bar represented as SD. ** $P<0.01$.

hydrogels ($0.10\text{cm}^3 \pm 0.04$) compared to the untreated controls ($0.7\text{cm}^3 \pm 0.27$) ($P=0.037$) (blank hydrogels group: $0.65\text{cm}^3 \pm 0.29$) (Figure 8D). Further proliferative and apoptotic staining suggested that M1 hydrogels reduced Ki-67 positive and increased TUNEL positive tumor cells indicating its tumor anti-proliferative and pro-apoptotic roles *in vivo* (Figure 8E).

Discussion

In the last decade, the advancement of biomaterial-based delivery systems in cancer therapies holds promising potentials^{13,14}. Studies using the biomaterials as carriers for delivering nanoparticles, chemotherapeutic drugs, antibodies, antigen specific peptides and immunological cells show beneficial results with increased efficacy compared to the direct injection approach¹⁴. In our

prior work, M1 macrophages have been experimented both *in vivo* and *in vitro* revealing their anti-tumor significances against HCC. Here we aimed at improving such novel therapeutic strategy by applying synthetic ECM biomaterial consisting of cross-linked PEGdA and Gel-PEG-Cys as a carrier for tumor-local delivery of activated M1 macrophages. As such, this innovative approach is the first of its kind in a biomaterial immunological combinatorial therapy for HCC.

In the present study, several novel insights with the advantages of the scaffold-based cancer immunotherapy over direct cell transfer were offered. First, we illustrated the anti-tumor activities of M1 hydrogels in both *in vitro* and *in vivo* studies. Apart from the dose and time-dependent effects on inhibiting HCC cells, *in situ* M1 hydrogels also significantly induced tumor necrosis and diminished tumor volume in two animal models. Second, the M1

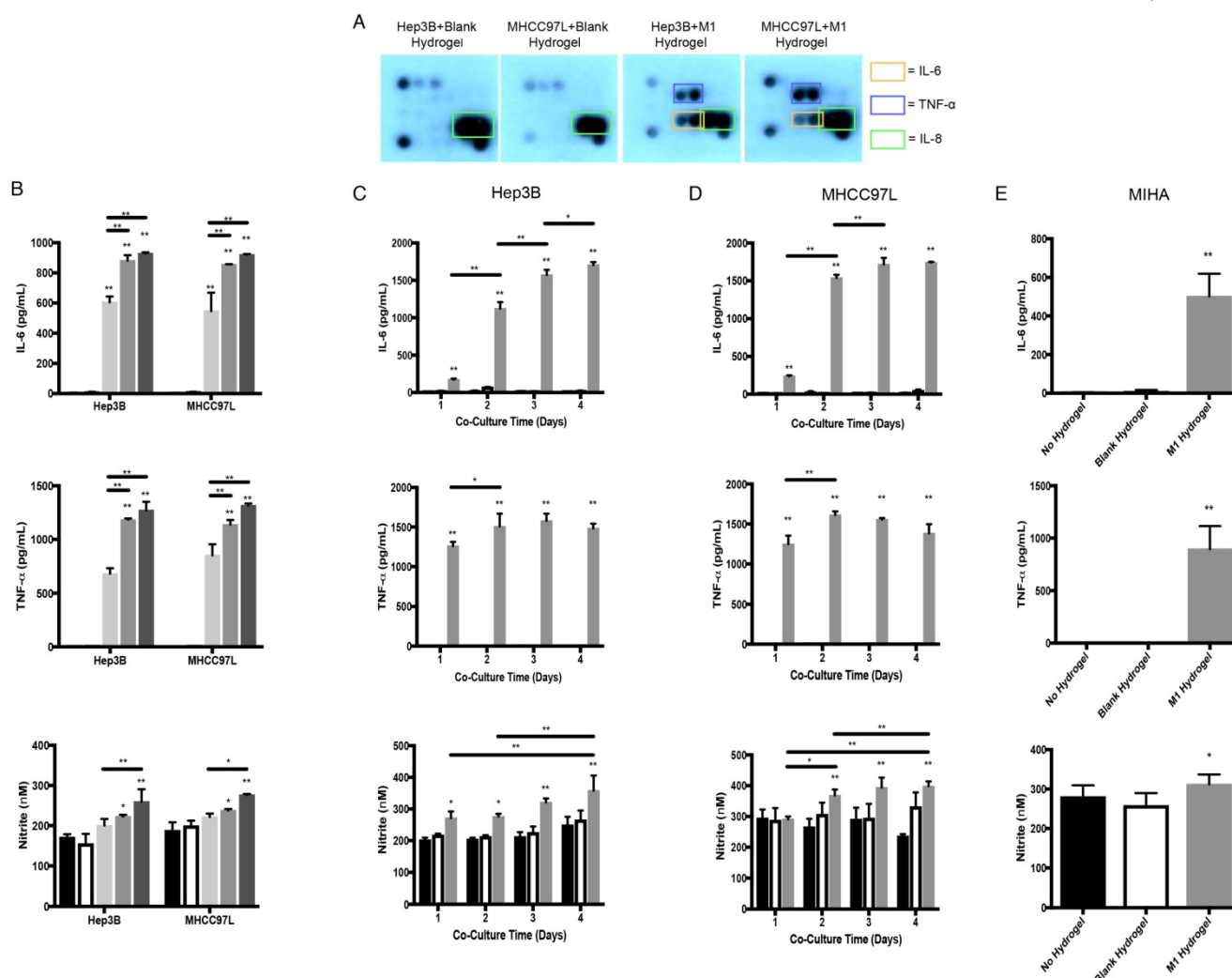


Figure 4. Cytokine secretion profiles and molecular analysis of the co-culture supernatants of M1 hydrogels with HCC and MIHA cells. (A) Cytokine secretion profiles of HCC cells and M1 hydrogel co-culture supernatants. (B) Level of IL-6, TNF-α, and nitrite of co-culture supernatants of HCC cells with no hydrogels (■), blank hydrogels (□) and hydrogels loaded with 2.5×10^5 (■), 5×10^5 (■), and 1×10^6 (■) M1 macrophages. The level of IL-6, TNF-α, and nitrite during 4 days co-cultivation of (C) Hep3B, (D) MHCC97L and (E) MIHA cells with no hydrogels (■), blank hydrogels (□) and hydrogels loaded with 5×10^5 M1 macrophages (■). The error bar represented as SD. *P<0.05, **P<0.01.

hydrogels displayed low immunogenicity, high biocompatibility and molecule release kinetics. In contrast to our previous direct portal vein injection approach, mice treated with M1 hydrogels did not show symptoms of acute inflammation or mortality while retaining the tumor killing phenotypes. Preliminary blood analysis showed that unlike the 1.5 fold increased of IL-1 α in the direct cell transfer group, the M1 hydrogels did not induce evaluation of the pro-inflammatory cytokine in circulation compared to untreated control. Third, M1 hydrogels exhibited minimum effects on non-tumorous hepatic cells showing its specificity towards tumors cells. Forth, we demonstrated the M1 activation of the gel-embedded monocytes with exogenous addition of IFN- γ and LPS. On the other hand, increased release of nitrite, IL-6 and TNF- α in the M1 hydrogels and HCC cells co-culture supernatants were found. These indicated that the permission for materials exchange, cell-to-cell interactions and signal transductions of the M1 hydrogel to its environment. Considering these advantages together with the ease of synthesis and formulation, it is very feasible to translate and extend

M1 hydrogels to clinical applications for HCC treatment.

For identifying the potential M1 derived tumor suppressive molecules and the underlying signal transduction pathway, we first confirmed that the M1 hydrogels up-regulated nitrite, IL-6, TNF- α and IDO1 upon the exposure to HCC cells. It was then shown that M1 hydrogel, TNF- α and nitrite caused HCC cell apoptosis via activating the caspase-3 signaling pathway. In addition, we discovered that up-regulation of IDO1 could be also induced by TNF- α in dose dependent manner (data not shown). It is reported that elevated nitrite levels can induce the cleavage and activation of caspase-3 with subsequent cleavage of PARP-1 that ultimately leads to apoptosis through a mitochondria-dependent death pathway²⁶⁻²⁷. Based on the current knowledge and experimental evidences, here we proposed an anti-tumor mechanism of M1 hydrogels. Increased levels of TNF- α during the treatment of M1 hydrogels to HCC cells promoted IDO1 expression in M1 macrophages leading to the secretion of nitrite and subsequently activated caspase-3 dependent apoptosis in the tumor cells (Figure 9).

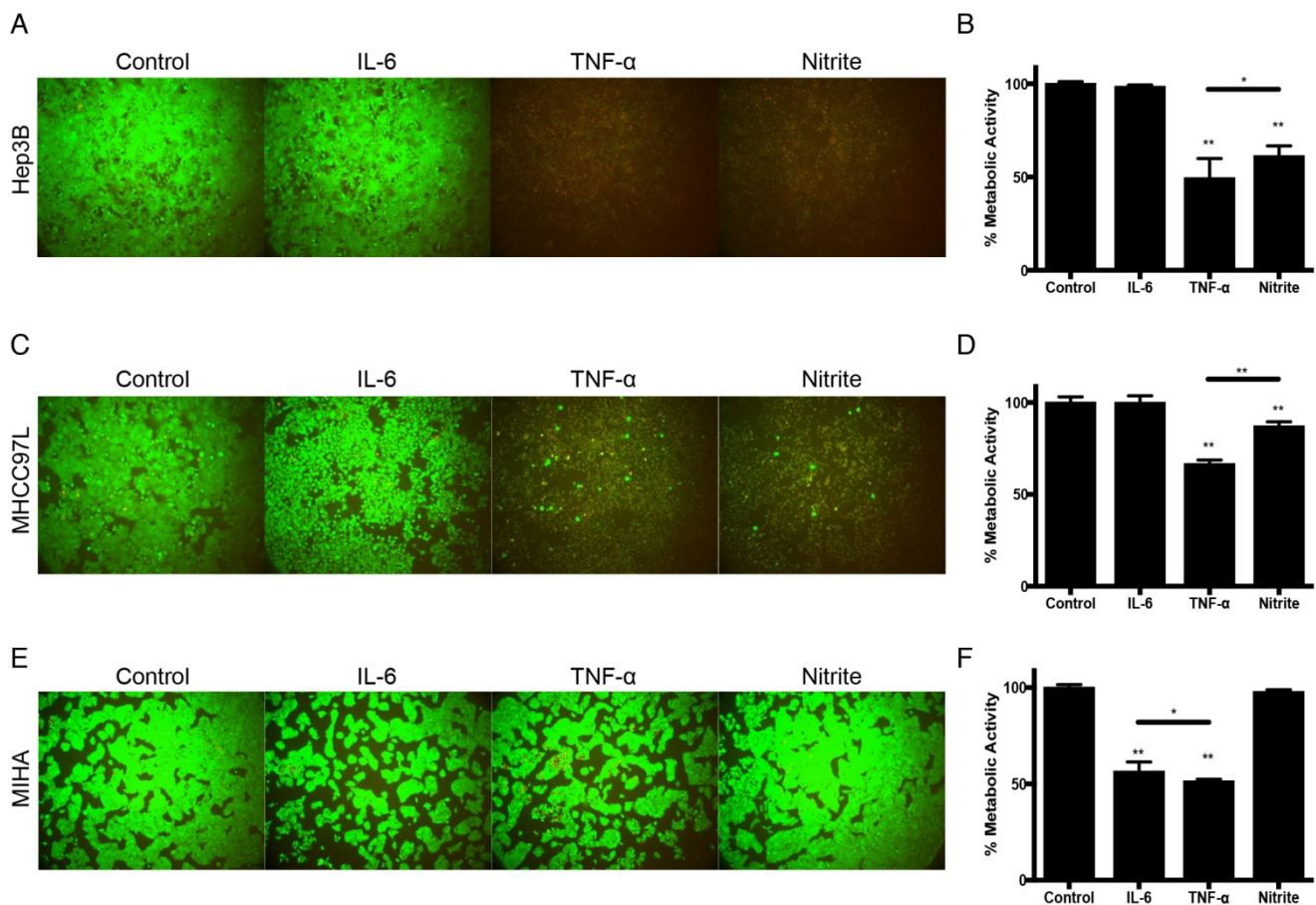


Figure 5. Tumor suppressive effects of IL-6, TNF- α and nitrite in HCC. (A) Hep3B live/dead images and (B) Corresponding normalized metabolic activity. (C) MHCC97L live/dead images and (D) Corresponding normalized metabolic activity. (E) MIHA live/dead images and (F) Corresponding normalized metabolic activity. The error bar represented as SD. *P<0.05, **P<0.01.

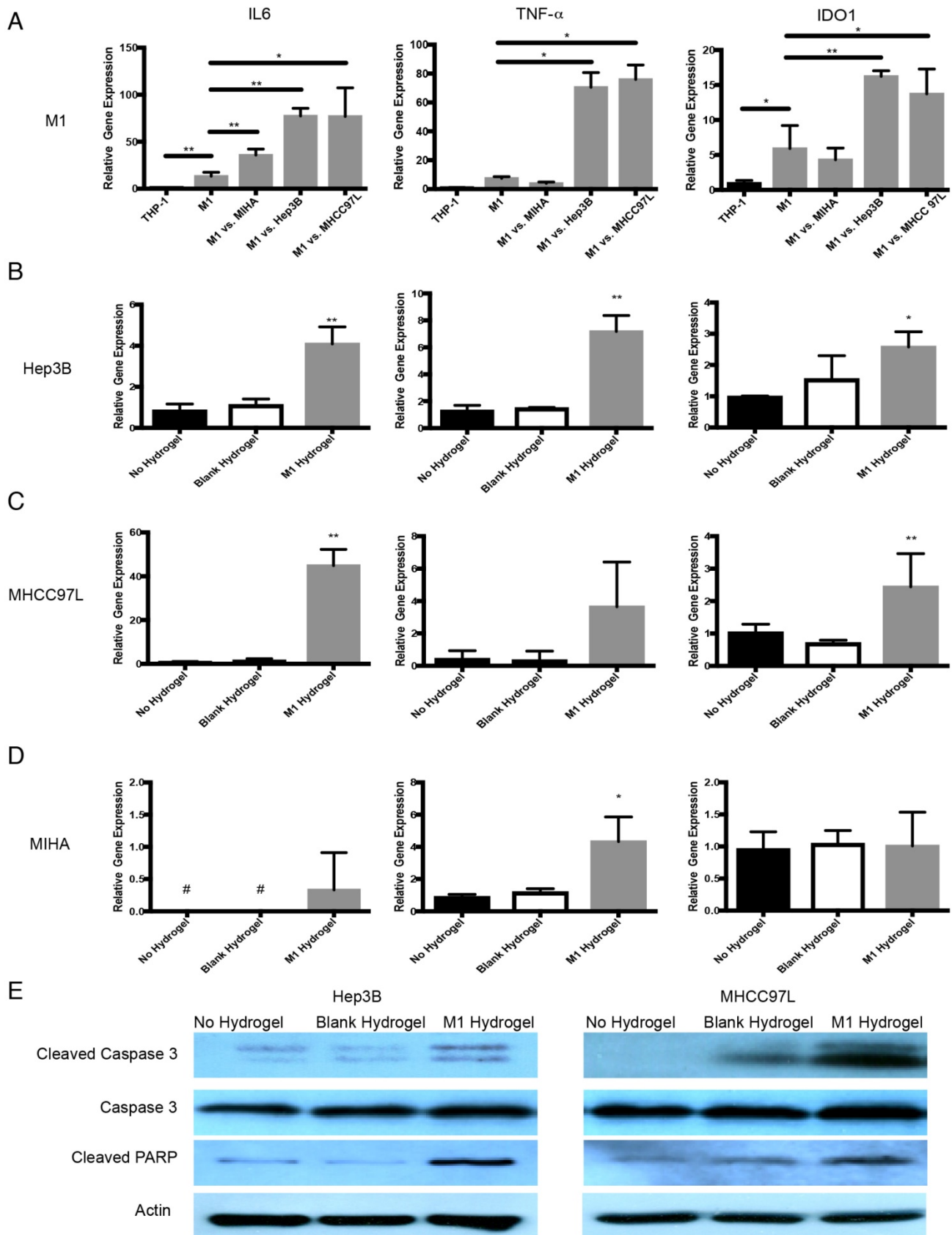


Figure 6. Anti-tumor molecular mechanism of M1 hydrogels against HCC. (A) Gene expression of *IL-6*, *TNF- α* , and *IDO1* in gels embedded M1 macrophages after coculture with Hep3B, MHCC97L and MIHA cells. Gene expression of *IL-6*, *TNF- α* , and *caspase-3* in (B) Hep3B, (C) MHCC97L, and (D) MIHA cells after co-culture with no hydrogels, blank hydrogels, and M1 hydrogels (5×10^5). (E) Western blot analyzes of cleaved caspase-3, caspase-3 and PARP in HCC cells after co-culture with no hydrogels, blank hydrogels and M1 hydrogels (5×10^5). The error bar represented as SD. * $P < 0.05$, ** $P < 0.01$.

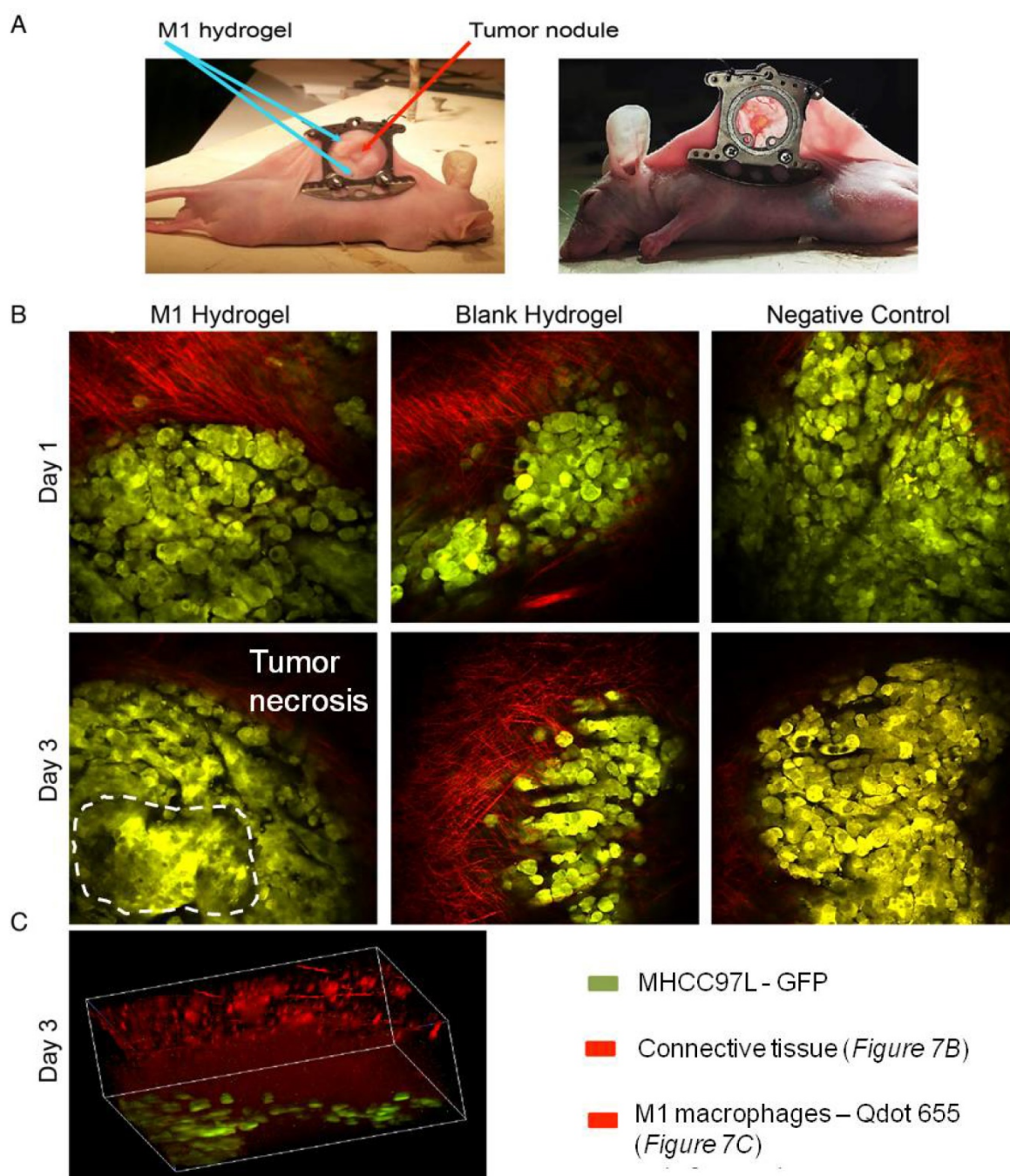


Figure 7. *In vivo* study of the anti-tumor effects of M1 hydrogels (1×10^6) in HCC tumors (MHCC97L-GFP) in a window-chamber model. **(A)** Window-chamber model setup of tumor nodule with the injection of polymerized M1 macrophage-loaded hydrogels. **(B)** Real-time intravital imaging of the tumors 1-3 days after the injection of M1 hydrogels. Tumor necrosis area indicated by white dashed line **(C)** Three-dimension reconstructed images of the injected site at day 3.

Interestingly, in contrast to TNF- α and nitrite, our study showed that up-regulation of IL-6 were not cytotoxic to HCC cells. Studies suggested that IL-6 autocrine production is critical for HCC progression acting as a risk indicator for adverse prognosis²⁸⁻²⁹. IL-6 enhances orosphere formation, p-STAT3 activation, survival, and self-renewal of human cancer stem cells (CSCs)³⁰. Recently, it is reported that tumor associated macrophages derived IL-6 is highly correlated with the occurrence and development of

HCC via activating anti-apoptotic STAT3 pathway³¹. In the present study, it is possible that the HCC cells attempted to utilize the M1 macrophage populations to assist in its own survival. Based on the findings, we speculated a paracrine feedback loop between M1 hydrogels and HCC cells for the pro- and anti-tumor phenotypes. Identifying such communications could be useful for mimicking the stimulatory signals and further enhancing the anti-tumor efficacy of the biomaterial.

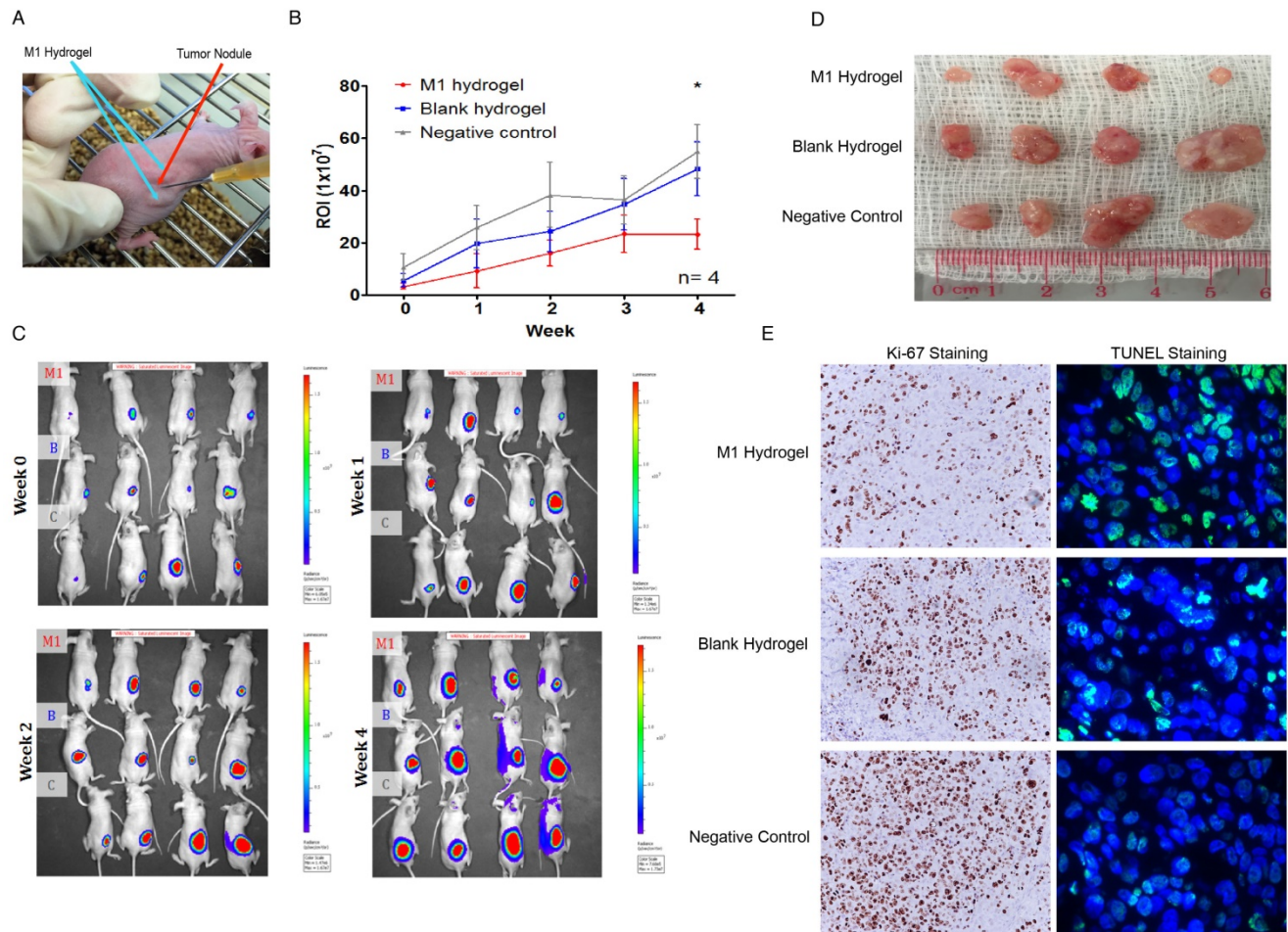


Figure 8. *In vivo* analysis of the anti-tumor effects of M1 hydrogels on tumor growth and histology of HCC tumors (MHCC97L-Luciferase) in a subcutaneous tumor model. (A) Subcutaneous tumor model setup of tumor module with the injection of polymerized M1 macrophage-loaded hydrogels adjacent to the tumor. (B) Measurements of mean *in vivo* subcutaneous tumor bioluminescence of each group over 4 weeks. Bioluminescent signals were quantified as photons/s at each imaging time point. (C) Monitoring of *in situ* tumor growth by PE IVIS Spectrum at week 1–4. Following euthanasia at week 4, (D) the examination of tumor volume. (E) Ki-67 and TUNEL staining of liver tumor tissues in each mouse. n = 4. *P<0.05. The error bar represented as SEM. M1: 1x10⁶ M1 macrophage loaded hydrogels; B: blank hydrogels; C: no hydrogels (control).

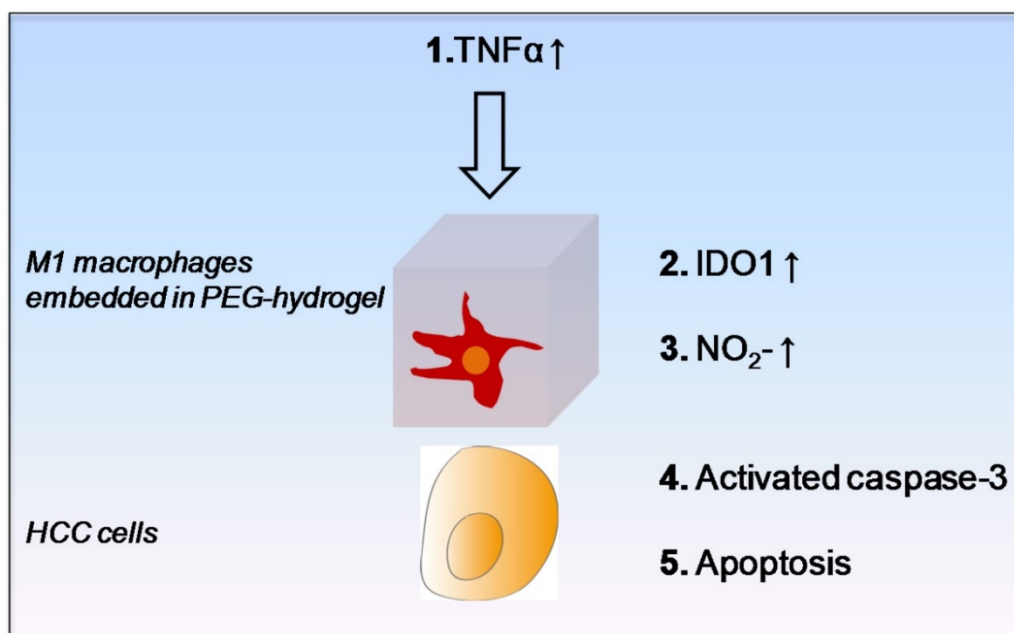


Figure 9. Schematic diagram of proposed anti-tumor molecular mechanism of M1 hydrogel.

In summary, we explored a new novel therapeutic strategy utilizing biomaterial engineering and immunology. The anti-tumor functionality, specificity and biocompatibility of M1 hydrogels were demonstrated both *in vitro* and *in vivo* studies. Localization of activated M1 macrophages to the tumor through encapsulation in hydrogels may provide an alternative and innovative treatment option against HCC.

Abbreviations

DWC: Dorsal window chamber

ECM: Extracellular matrix

HCC: Hepatocellular carcinoma

IDO1: Indoleamine-pyrrole 2,3-dioxygenase

IL-6: Interleukin 6

IFN- γ : Interferon gamma

LPS: Lipopolysaccharide

MSC: Mesenchymal stromal/stem cells

NK cells: Natural killer cells

PEGdA: Poly(ethylene glycol) diacrylate

Gel-PEG: Cys - Thiolated gelatin poly(ethylene glycol)

TNF- α : Tumor necrosis factor alpha

Supplementary Material

Additional File 1:

Supplemental Figure 1.

<http://www.thno.org/v07p3732s1.pdf>

Additional File 2:

Supplemental Video 1.

<http://www.thno.org/v07p3732s2.avi>

Acknowledgement

This study was supported by the Collaborative Research Fund (HKU3/CRF/11R & C7027-14GF) and General Research Funding (75011M, 17115515 & 17115614) of the Research Grant Council, Hong Kong; A National Science Foundation of China (NSFC) grant (No.81470903 & 81572945); Health and Medical Research Funding (HMRF) (No. 03143336 & 14131012) and NIH Biotechnology Training Program (GM008349).

Competing Interests

The authors have declared that no competing interest exists.

References

- [No authors listed]. EASL-EORTC Clinical Practice Guidelines: Management of hepatocellular carcinoma. *J Hepatol.* 2012; 56: 908-43.
- Greten TF, Wang XW, Korangy F. Current concepts of immune based treatments for patients with HCC: from basic science to novel treatment approaches. *Gut.* 2015; 64: 842-8.
- Ruella M, Kalos M. Adoptive immunotherapy for cancer. *Immunol Rev.* 2014; 257: 14-38.
- Porter DL, Levine BL, Kalos M et al. Chimeric antigen receptor-modified T Cells in chronic lymphoid leukemia. *N Engl J Med.* 2011; 365: 725-33.

- Grupp SA, Kalos M, Barrett D, et al. Chimeric antigen receptor-modified T cells for acute lymphoid leukemia. *N Engl J Med.* 2013; 368: 1509-18.
- Miller JS, Soignier Y, Panoskalis-Mortari A, et al. Successful adoptive transfer and *in vivo* expansion of human haploidentical NK cells in patients with cancer. *Blood.* 2005; 105: 3051-7.
- Geller MA, Cooley S, Judson PL, et al. A phase II study of allogeneic natural killer cell therapy to treat patients with recurrent ovarian and breast cancer. *Cytotherapy.* 2010; 13: 98-107.
- Bachanova V, Burns LJ, McKenna DH, et al. Allogeneic natural killer cells for refractory lymphoma. *Cancer Immunol Immunother.* 2010; 59(11):1739-44.
- Mills CD, Lenz LL, Harris RA. A Breakthrough: macrophage-directed cancer immunotherapy. *Cancer Res.* 2016; 76: 513-6.
- Mantovani A, Sozzani S, Locati M, et al. Macrophage polarization: tumor-associated macrophages as a paradigm for polarized M2 mononuclear phagocytes. *Trends Immunol.* 2002; 23: 549-55.
- O'Sullivan T, Saddawi-Konefka R, Vermi W, et al. Cancer immunoediting by the innate immune system in the absence of adaptive immunity. *J Exp Med.* 2012; 209: 1869-82.
- Yeung WHO, Lo CM, Ling CC, et al. Alternatively activated (M2) macrophages promote tumor growth and invasiveness in hepatocellular carcinoma. *J Hepatol.* 2015; 62: 607-16.
- Singh A, Peppas NA. Hydrogels and scaffolds for immunomodulation. *Adv Mater.* 2014; 26(38): 6530-6541.
- Gu L, Mooney DJ. Biomaterials and emerging anticancer therapeutics: engineering the microenvironment. *Nat Rev Cancer.* 2016; 16: 56-66.
- Burmania JA, Stevens KR, Kao WJ. Cell interaction with protein-loaded interpenetrating networks containing modified gelatin and poly(ethylene glycol) diacrylate. *Biomaterials.* 2003; 24: 3921-30.
- Xu K, Fu Y, Chung W, et al. Thiol-ene-based biological/synthetic hybrid biomatrix for 3-D living cell culture. *Acta Biomater.* 2012; 8: 2504-16.
- Cantu DA, Hematti P, Kao WJ. Cell encapsulating biomaterial regulates mesenchymal stromal/stem cell differentiation and macrophage immunophenotype. *Stem Cells Transl Med* 2012; 1: 740-9.
- Fu Y, Xu K, Zheng X, et al. 3D cell entrapment in crosslinked thiolated gelatin-poly(ethylene glycol) diacrylate hydrogels. *Biomaterials.* 2012; 33: 48-58.
- Wang C, Varshney RR, Wang DA. Therapeutic cell delivery and fate control in hydrogels and hydrogel hybrids. *Adv Drug Deliv Rev.* 2010; 62: 699-710.
- Xu K, Cantu DA, Fu Y, et al. Thiol-ene Michael-type formation of gelatin/poly(ethylene glycol) biomatrices for three-dimensional mesenchymal stromal/stem cell administration to cutaneous wounds. *Acta Biomater.* 2013; 9: 8802-14.
- Kleinbeck KR, Bader RA, Kao WJ. Concurrent *in vitro* release of silver sulfadiazine and bupivacaine from semi-interpenetrating networks for wound management. *J Burn Care Res.* 2009; 30: 98-104.
- Guerra AD, Cantu DA, Vecchi JT, et al. Mesenchymal stromal/stem cell and minocycline-loaded hydrogels inhibit the growth of staphylococcus aureus that evades immunomodulation of blood-derived leukocytes. *AAPSJ.* 2015; 17: 620-30.
- Cantu DA, Hematti P, Kao WJ. Cell encapsulating biomaterial regulates mesenchymal stromal/stem cell differentiation and macrophage immunophenotype. *Stem Cells Transl Med.* 2012; 1: 740-9.
- Guerra AD, Rose WE, Hematti P, et al. Minocycline enhances the mesenchymal stromal/stem cell pro-healing phenotype in triple antimicrobial-loaded hydrogels. *Acta Biomater.* 2017; 51: 184-196.
- Qi X, Ng KT, Shao Y, et al. The clinical significance and potential therapeutic role of gpx3 in tumor recurrence after liver transplantation. *Theranostics.* 2016; 6: 1934-46.
- Fulda S. Targeting apoptosis for anticancer therapy. *Semin Cancer Biol.* 2015; 31: 84-8.
- Qiu M, Chen L, Tan G, et al. A reactive oxygen species activation mechanism contributes to JS-K-induced apoptosis in human bladder cancer cells. *Sci Rep.* 2015; 5: 15104.
- Porta C, De Amici M, Quaglini S, et al. Circulating interleukin-6 as a tumor marker for hepatocellular carcinoma. *Ann Oncol.* 2008; 19: 353-8.
- Soresi M, Giannitrapani L, D'Antona F, et al. Interleukin-6 and its soluble receptor in patients with liver cirrhosis and hepatocellular carcinoma. *World J Gastroenterol.* 2006; 12: 2563-848.
- Krishnamurthy S, Dong Z, Vodopyanov D, et al. Endothelial cell-initiated signaling promotes the survival and self-renewal of cancer stem cells. *Cancer Res.* 2010; 70: 9969-9978.
- Kong L, Zhou Y, Bu H, et al. Deletion of interleukin-6 in monocytes/macrophages suppresses the initiation of hepatocellular carcinoma in mice. *J Exp Clin Cancer Res.* 2016; 35(1): 131.